Title

Construction and characterization of a knock-down RNA interference line of OsNRPD1 in rice (Oryza sativa ssp japonica cv Nipponbare).

Journal

Philosophical Transactions of the Royal Society of London. Biological Sciences, 375(1795)

Authors

Debladis, Emilie

Lee, Tzuu-Fen

Huang, Yan-Jiun

et al.

Publication Date

2020-03-30

DOI

10.1098/rstb.2019.0338

Peer reviewed

PHILOSOPHICAL TRANSACTIONS B

royalsocietypublishing.org/journal/rstb

Research

Cite this article: Debladis E *et al*. 2020 Construction and characterization of a knock-down RNA interference line of *OsNRPD1* in rice (*Oryza sativa* ssp *japonica* cv Nipponbare). *Phil. Trans. R. Soc. B* **375**: 20190338.
http://dx.doi.org/10.1098/rstb.2019.0338

Accepted: 26 July 2019

One contribution of 15 to a discussion meeting issue 'Crossroads between transposons and gene regulation'.

Subject Areas:
genomics, molecular biology

Keywords:
polymerase IV, RNA-dependent DNA methylation, transposable elements, RNA interference

Author for correspondence:
Eric Lasserre
e-mail: eric.lasserre@univ-perp.fr

Electronic supplementary material is available online at https://doi.org/10.6084/m9.figshare.c.4796271.

THE ROYAL SOCIETY PUBLISHING

Construction and characterization of a knock-down RNA interference line of *OsNRPD1* in rice (*Oryza sativa* ssp *japonica* cv Nipponbare)

Emilie Debladis[1,2], Tzuu-Fen Lee[4], Yan-Jiun Huang[5], Jui-Hsien Lu[5], Sandra M. Mathioni[4], Marie-Christine Carpentier[1,2], Christel Llauro[1,2], Davy Pierron[1,2], Delphine Mieulet[6], Emmanuel Guiderdoni[6], Pao-Yang Chen[5], Blake C. Meyers[4,7], Olivier Panaud[1,2,3] and Eric Lasserre[1,2]

[1]Laboratoire Génome et Développement des Plantes, Université de Perpignan Via Domitia, 52, Avenue Paul alduy, 66860 Perpignan Cedex, France
[2]Laboratoire Génome et Développement des Plantes, Centre National de la Recherche Scientifique, 52, Avenue Paul alduy, 66860 Perpignan Cedex, France
[3]Institut Universitaire de France, Paris, France
[4]Donald Danforth Plant Science Center, St Louis, MO 63132, USA
[5]Institute of Plant and Microbial Biology, Academia Sinica, Taipei 11529, Taiwan
[6]CIRAD, UMR AGAP, F34398 Montpellier Cedex 5, France
[7]Division of Plant Sciences, University of Missouri-Columbia, Columbia, MO 65211, USA

ED, 0000-0003-4734-7426; SMM, 0000-0002-8853-4108; M-CC, 0000-0002-4795-9054; EG, 0000-0003-2760-2864; P-YC, 0000-0002-7402-3075; BCM, 0000-0003-3436-6097; OP, 0000-0002-9292-503X; EL, 0000-0002-1408-2612

In plants, RNA-directed DNA methylation (RdDM) is a silencing mechanism relying on the production of 24-nt small interfering RNAs (siRNAs) by RNA POLYMERASE IV (Pol IV) to trigger methylation and inactivation of transposable elements (TEs). We present the construction and characterization of *osnrpd1*, a knock-down RNA interference line of *OsNRPD1* gene that encodes the largest subunit of Pol IV in rice (*Oryza sativa* ssp *japonica* cv Nipponbare). We show that *osnrpd1* displays a lower accumulation of *OsNRPD1* transcripts, associated with an overall reduction of 24-nt siRNAs and DNA methylation level in all three contexts, CG, CHG and CHH. We uncovered new insertions of known active TEs, the LTR retrotransposons *Tos17* and *Lullaby* and the long interspersed nuclear element-type retrotransposon *Karma*. However, we did not observe any clear developmental phenotype, contrary to what was expected for a mutant severely affected in RdDM. In addition, despite the presence of many putatively functional TEs in the rice genome, we found no evidence of *in planta* global reactivation of transposition. This knock-down of *OsNRPD1* likely led to a weakly affected line, with no effect on development and a limited effect on transposition. We discuss the possibility that a knock-out mutation of *OsNRPD1* would cause sterility in rice.

This article is part of a discussion meeting issue 'Crossroads between transposons and gene regulation'.

1. Background

The DNA of flowering plants as a whole is predominantly made up of transposable elements (TEs), mobile genetic units able to proliferate in their host genomes. First described by B. McClintock more than 60 years ago, they are grouped into two classes based on their transposition mechanisms: class I elements or retrotransposons transpose via an RNA-mediated copy-and-paste mechanism whereas class II elements or DNA transposons transpose without using an RNA intermediate [1,2]. LTR retrotransposons (LTR-RTs) are the most abundant in plants. Non-LTR-RTs include long interspersed

nuclear elements (LINEs) and short interspersed nuclear elements (SINEs) [3].

TEs have been shown to be one of the most important factors driving the structure, function and evolution of eukaryotic genomes [4–6]. However, because of their combined mutagenic and replicative properties, they also may threaten the overall structure and function of the genome of their host. A balance between both consequences has been reached: host organisms have evolved strong controls of transposition that allowed the taming of TE proliferation while keeping transposition possible. Young TE copies are thus silenced by epigenetic marks such as cytosine methylation, ensuring a stable repression of TE expression and preventing their proliferation [7]. This *de novo* DNA methylation can be initiated via the RNA-directed DNA methylation (RdDM) mechanism, a plant-specific pathway through which small interfering RNAs (siRNAs) target homologous DNA regions through base-pairing to methylate them. The RdDM pathway is well characterized in *Arabidopsis thaliana* [8,9]. The canonical one is initiated by the RNA POLYMERASE IV (Pol IV), which generates a single strand RNA of the target locus that is a template for RNA-DEPENDENT RNA POLYMERASE 2 (Pol II) to generate a double strand RNA (dsRNA). Then, DICER-LIKE 3 cleaves these dsRNA into 24 nucleotides siRNAs (24 nt siRNA) one strand of which is loaded into ARGONAUTE 4, which can target nascent scaffold RNA POLYMERASE V (Pol V) transcripts or genomic DNA (gDNA) by base-pairing. Finally, this targeting leads to the recruitment of the DNA methyltransferase DOMAINS REARRANGED METHYLTRANSFERASE 2 to mediate *de novo* methylation in all three different sequence contexts, CG, CHG and CHH, where H is A, C or T [10]. However, *de novo* methylation of cytosines in the CHH context is the specific hallmark of RdDM since methylation at the symmetrical CG and CHG sites can be maintained at each round of replication by METHYLTRANSFERASE 1 and CHROMOMETHYLASE 3, respectively [11].

In addition to the canonical pathway, Pol II expression-dependent forms of RdDM that partly incorporate components typically associated with post-transcriptional gene silencing have recently been identified in *A. thaliana* [9,12].

In rice (*Oryza sativa* ssp *japonica*), TEs account for at least 35% of the genome [13]. Despite evidence of many polymorphic insertions of TEs in different accessions or cultivars of the same species [14,15], showing that *in planta* transposition was ongoing in the field, very few transposition events could be triggered and observed in laboratory conditions. This was the case for three LTR-RTs, namely *Tos17* [16], *Lullaby* [17] and *Karma* [18], and two related DNA transposons, *mPing* and *Pong* [19,20]. However, transposition of these elements did not occur *in planta* but was triggered by an intermediate step of long-term *in vitro* culture of cells or anthers. Only some mutants affected in methylation of histones [21] or DNA [22,23] have been shown to display transposons reactivation *in planta*.

Recent advances have shed light on epigenetic regulation and the epigenomic landscape in rice [7]. Key actors of DNA methylation have been characterized [23–26]. However, only few genes have been fully identified as actors in the RdDM mechanism. OsDCL3a is the rice DICER-LIKE 3 homologue involved in 24-nt siRNA processing [26]. Reduction of OsDCL3a function reduced the 24-nt siRNAs predominantly from Miniature Inverted-repeat Transposable Elements (MITEs) and elevated expression of nearby genes involved in the homeostasis of the plant hormones gibberellin and brassinosteroid. The o*sdcl3a* RNAi lines thus displayed several developmental alterations compared to wild-type (WT). Disruption of *OsDRM2*, coding the rice methyltransferase responsible for *de novo* methylation, led to an 85% decrease in CHH methylation and impaired both vegetative and reproductive development [24,27]. However, since none of these studies focused on transposition, nothing is known about the impact of those mutations, and by extension RdDM, on TEs mobilization in rice.

Foremost among these factors and central to the mechanism of RdDM, as described above for *Arabidopsis*, is the Pol IV because it is needed to produce the siRNA trigger for methylation. Pol IV is a large holoenzyme composed of 12 subunits [28]. NRPD1 is the largest one and is derived from the duplication of Pol II subunit NRPB1. It is specific to Pol IV and a component of the catalytic centre [28]. Two orthologues of NRPD1 have been identified in rice [29] and present the same domain structure as in *A. thaliana*, suggesting a similar molecular function.

Interestingly, however, no knock-out mutant has been described for any of the primary components of the RdDM pathway, Pol IV and Pol V in rice, suggesting that they could be lethal [30], in contrast to what occurs in *Arabidopsis*. This is further supported by the observation that mutations in genes encoding other RdDM factors strongly affected rice development [24,26,27] when their counterparts in *Arabidopsis* did not show obvious defects [8].

In this paper, we describe the construction and the characterization of *osnrpd1*, a knock-down RNAi line of *OsNRPD1* gene. Our initial goal was to create a rice line with a broadly relaxed epigenetic control over TEs to study their transcriptional regulation. OsNRPD1, being of central importance in producing the siRNA triggers that keep TEs silent, was a target of choice. *osnrpd1* did not display any obvious growing defects but we show that 24-nt small RNAs are under-accumulated and that the methylation of cytosine residues in all contexts is reduced compared to WT plants. However, while we observed new insertions of three known active retrotransposons, namely *Tos17*, *Lullaby* and *Karma*, *OsNRPD1* knock-down was not sufficient to broadly trigger transposition of many putatively functional TEs populating the rice genome.

2. Methods

(a) Plant material

Oryza sativa ssp. *japonica* cv. Nipponbare rice plants and the derived *osnrpd1* RNAi line were obtained from CIRAD, Montpellier, France. They were cultivated in a growth chamber (Percival) under a 12 h light–dark cycle (12 h–28°C/12 h–26°C) and with a relative humidity of 80% during the day and 70% during the night. The light intensity varied gradually over 40 min at the beginning and end of the day.

For the construction of *osnrpd1*, a 150 nucleotides-long fragment belonging to a region coding for the RNAP_IV_NRPD1 C-terminal conserved domain of NCBI Gene *LOC4336722* (nucleotides 3886–4036) was amplified by PCR (primers are described in electronic supplementary material, table S5, additional file 5) and cloned into the hpRNA binary vector pBIOS738 as described in electronic supplementary material, figure S1.

To generate the *osnrpd1* RNAi line, an *Agrobacterium*-mediated transformation of mature seed embryo-derived callus was performed as previously described [31]. The one T-DNA-containing T0 regenerated plants, 6.2, 8.1, 20.1 and 23.1 were selected (figure 1). Further generations of single-seed descents have been obtained by selfing.

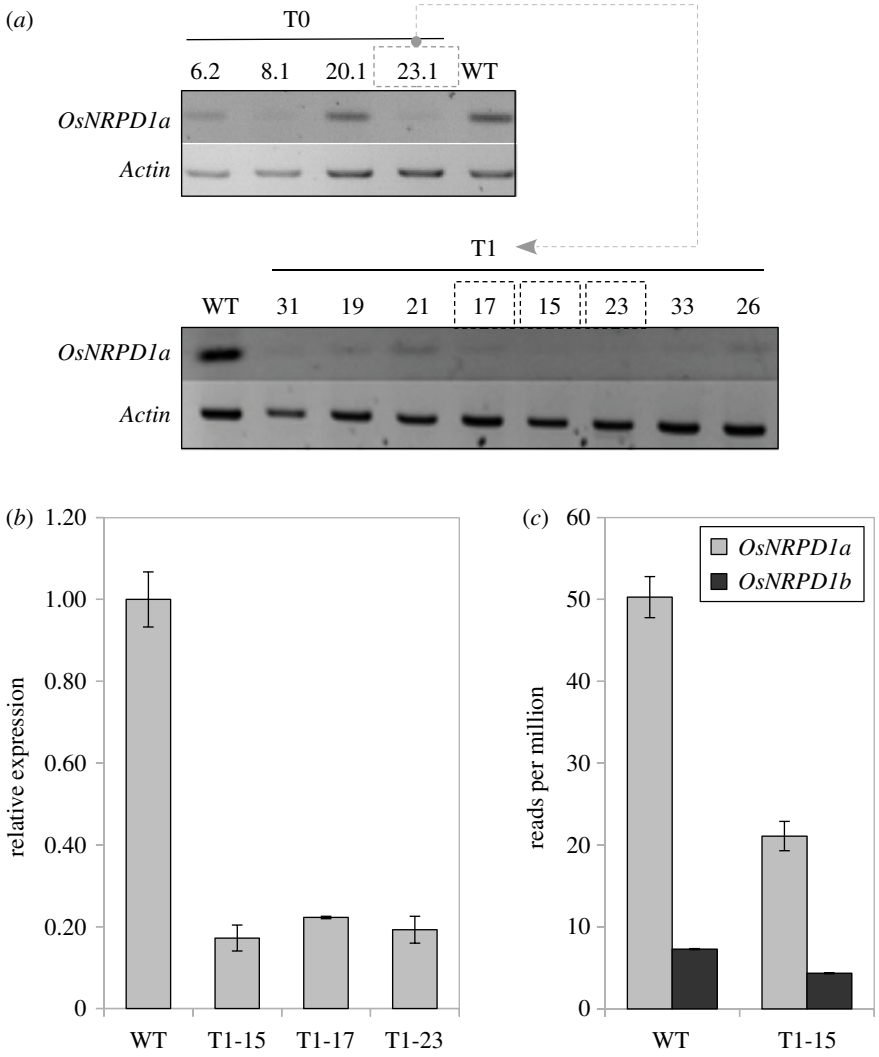

Figure 1. Transcript accumulation of *OsNRPD1* genes is lower in the *osnrpd1* mutants. (*a*) Top, semi-quantitative RT-PCR analysis of *OsNRPD1a* transcripts accumulation in four T0 regenerants (6.2, 8.1, 20.1 and 23.1) and the wild-type progenitor (WT). Bottom, same analysis in 8 T1 individuals of the T0-23.1 progeny after selfing. The dashed frames indicate the plants that displayed a strong reduction in transcripts accumulation and that have been selected and further described in this study. (*b*) RT-qPCR analysis of *OsNRPD1a* transcripts accumulation level relative to *ACTIN* (ΔΔCt method) in three selected T1 plants (T1-15, T1-17 and T1-23) compared to WT, three biological replicates each, confirming the results above. (*c*) *OsNRPD1* transcripts accumulation in T1-15 after RNA-Seq analysis showing, based on three biological replicates, that both genes are affected. Error bars represent the standard deviation.

(b) DNA and RNA extraction

For DNA-seq and PCR analysis, total DNA was extracted from 50 mg of frozen leaves harvested from one-month-old plants by a CTAB-based method as previously described [32].

For RNA-seq and RT-PCR analysis, total RNA was extracted from 50 mg of leaves using the TRIzol reagent (Invitrogen Life Technologies) and treated with DNAse I (RQ1 RNase-Free DNase, Promega). RNAs were checked on 1% agarose gels and quantified using a Qubit® RNA Assay Kit in a Qubit® 2.0 Fluorometer (Life Technologies).

(c) PCR and RT-PCR methods

For PCR analysis of *Tos17* insertions, 20 ng of total DNA were used. Thirty cycles of PCR amplifications were performed with a hybridization step at 58°C.

For semi-quantitative RT-PCR analysis of *OsNRPD1a* and *ACTIN* transcripts accumulation, cDNAs were synthesized from 800 ng of isolated RNA using an oligonucleotide dT primer and the GoScript reverse transcriptase (Promega). Twenty-four cycles of PCR amplifications were performed with a hybridization step at 58°C.

Analyses by quantitative real-time PCR (qRT-PCR) were established using 7–35 ng of cDNA, synthesized as described above. qRT-PCRs were run on a LightCycler 480 (Roche) using Takyon No Rox SYBR MasterMix dTTP Blue Kit (Eurogentec). The qRT-PCR conditions were the following: a first denaturation step at 95°C for 5 min followed by 40 cycles at 95°C for 15 s, an annealing and elongation step at 60°C for 60 s, and a melting curve analysis at 95°C for 10 s, 60°C for 10 s, an increase of 0.04°C per second until 95°C and a final step of cooling at 40°C for 30 s. Primers were used at a concentration of 2 µM. Three biological replicates were analysed for each plant. *OsNRPD1* expression level relative to *ACTIN* was calculated using the ΔΔCt method.

All primers sequences are listed in electronic supplementary material, table S5, additional file 5.

(d) DNA-seq and read mapping

DNA quality and concentration were determined using a high sensitivity DNA Bioanalyzer chip (Agilent Technologies). Three hundred and fifty base pairs DNA libraries have been prepared using Illumina's PCR-free DNA kit and sequenced at 2 × 102 nt or 2 × 151 nt on a Hiseq2500 instrument (HudsonAlpha Genome Sequencing Center, Huntsville, USA). Quality control of FASTQ

files was evaluated using the FastQC tool (v. 0.10.1 www.bioinformatics.babraham.ac.uk/projects/fastqc). To remove any read originating from organelle genomes, reads were mapped against the mitochondria (GenBank NC_011033) and chloroplast genomes (GenBank X15901) using the program BOWTIE2 v. 2.2.2 [33] with sensitive-local mapping. Unmapped reads were then considered for the systematic search of TEs insertions as described in electronic supplementary material, additional file 6.

(e) RNA-seq and *OsNRPD1* transcript accumulation

Six stranded cDNA libraries (WT and T1-15, three biological replicates each) from poly-A-enriched RNAs were generated using Illumina's stranded RNAseq kit and sequenced at 2 × 102 nt on a Hiseq 2500. Quality control of FASTQ files was made as for DNA-seq. Analysis of transcript accumulation of *OsNRPD1a* and *OsNRPD1b* was performed as follows: a BOWTIE2 index was done for each mRNA sequence. Then, reads from the six libraries were mapped on both sequences using BOWTIE2 in the default mode with the no-unal option to suppress SAM records for reads that failed to align. SAMTOOLS utilities [34] were then used to select and count concordant alignments with no mismatches. Since many transcripts were produced from the inverted repeat of *osnrpd1*, those reads that mapped to the 150 bp region that was used for the RNAi construct were removed in each analysis.

(f) sRNA-seq and mapping

Total RNA from the materials described above was isolated using Tri Reagent™ (Molecular Research Center). Small RNA libraries were constructed using the Illumina TruSeq Small RNA Sample Preparation Kit, and sequenced on an Illumina HiSeq2000 instrument. Raw sequencing data were first trimmed of adapter sequences, with trimmed lengths between 18 and 34 nt. The read counts were normalized based on the total abundance of genome-matched reads, excluding structural sRNAs originating from annotated tRNA, rRNA, small nuclear and small nucleolar RNAs. The 21-nt reads that mapped to the 150 bp region targeted by the inverted repeat of the RNAi construct were removed in each analysis. Read counts were normalized to 20 M reads per library as well as to total genome-matched reads.

To assess regions of *OsNRPD1a* targeted by siRNAs, reads were aligned to the variant 6 of *OsNRPD1a* mRNA with BOWTIE. Only reads with perfect match were kept. Coverage at each nucleotide was calculated.

(g) Genome-wide methylome profiling by methylC-seq

For methylC-seq library construction, 200 ng of RNA-free gDNA were used for library construction following a protocol previously described with some variations [35]. Briefly, gDNA in TE buffer was fragmented in a Covaris focused ultrasonicator to generate approximately 200 bp fragments. The fragmented gDNA was kit-purified (QIAquick PCR purification kit, Qiagen), end-repaired (End-It DNA end repair kit, Epicentre), and 'A' bases were added to the 3′ end of DNA then kit-purified again. Next, the methylated adapters were ligated to DNA fragments using Fast-Link™ DNA ligation kit (Epicentre) then kit-purified. 250–500 bp DNA fragments in the ligated products were extracted from a 2% agarose gel (BioRad) and purified (QIAquick Gel Extraction Kit, Qiagen). The adaptor-ligated gDNA was treated with sodium bisulfite for cytosine conversion with the MethylCode kit (Life Technologies). The bisulfite-converted gDNA was then amplified by PCR using Pfu Turbo Cx Hotstart DNA polymerase and PCR programme as described in the above-mentioned paper, with 14 cycles of amplification. The amplified library was purified using Agencourt Ampure XP beads (Bechman-Coulter) and sequenced with Illumina technology. Bisulfite converted reads were aligned to the rice reference genome (IRGSP1.0) using BS-Seeker2 with default parameters [36]. Genome-wide DNA methylation profiles were generated by determining methylation levels for each cytosine in the genome. We only included cytosines that are covered by at least four reads. We estimated the bisulfite conversion rate with respect to rice chloroplast genome: 96.35% for WT, 97.25% for T0, 98.04% for T1-15 and 97.21% for T1-23. BS-seq libraries and mapping data are presented in electronic supplementary material, additional file 3.

3. Results

(a) Design of the *osnrpd1* RNAi construct

Two orthologues of *NRPD1* were identified in rice, corresponding to NCBI Gene IDs *LOC4336722* and *LOC4347810*, both giving rise to several variants (electronic supplementary material, figure S1, additional file 1). Hereafter, the corresponding genes or transcripts will be named *OsNRPD1a* and *OsNRPD1b*, respectively, and collectively named *OsNRPD1*. Because we could not identify a viable insertional mutant of *OsNRPD1a* from the available collections (see §4), we used an RNAi strategy to post-transcriptionally inactivate both *OsNRPD1* genes. We selected a 150 nucleotides-long fragment belonging to a region coding for the RNA-P_IV_NRPD1 C-terminal conserved domain of the locus LOC4336722, characteristic of NRPD1 proteins that diverged from NRPB1 of Pol II [37]. Both mRNAs are 93% identical in this region (electronic supplementary material, figure S1, additional file 1). This fragment was cloned into a binary vector in the form of two inverted repeats separated by an intron and inserted into the genome of a *Oryza sativa* cv. Nipponbare plant by transformation with *Agrobacterium tumefaciens* (electronic supplementary material, figure S1, additional file 1). One T0 regenerant and a progeny of three T1 plants obtained by self-propagation (named T1-15, T1-17, T1-23), homozygous for the T-DNA insertion harbouring the RNAi construct, were the objects of this study.

(b) The accumulation of *OsNRPD1* transcripts is drastically lowered

The T0 regenerant described in this study (plant 23.1 on figure 1*a*) had been selected among four and self-propagated because it displayed the lowest expression level of *OsNRPD1a* based on semi-quantitative RT-PCR analysis (figure 1*a*). Three T1 plants (T1-15, T1-17 and T1-23), displaying the lowest accumulation of the *OsNRPD1a* transcript, were then selected (figure 1*a*). The lower accumulation of the *OsNRPD1a* transcript was confirmed on T1-15, T1-17 and T1-23 by RT-qPCR (figure 1*b*). We also obtained RNA-Seq data from T1-15. These data confirmed that the accumulation of the *OsNRPD1a* transcript was lower in the mutant (figure 1*c*). In addition, they showed that the *OsNRDP1b* transcripts were much less accumulated than the *OsNRPD1a* ones and, more importantly, that the RNAi construct was able to reduce the accumulation of both (figure 1*c*). This lower abundance of *OsNRPD1a* transcripts in the RNAi lines is in agreement with the precise targeting of *OsNRPD1a* gene by 21-nt siRNAs at the 150-nt long region used to devise the RNAi construct (electronic supplementary material, figure S2, additional file 1).

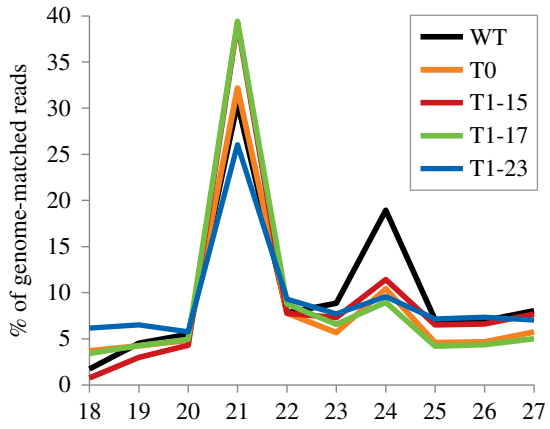

Figure 2. Accumulation of 24-nt small RNAs is lowered in the *osnrpd1* mutants. Small RNA size profiles in wild-type (WT) and *osnrpd1* mutants (T0 and three T1 plants), normalized to total genome-matched read. For each size class, siRNA abundance was calculated as a percentage of the sum of abundances of total genome-matched reads.

(c) The accumulation of 24-nt siRNAs is lowered

Since OsNRPD1 is a subunit of the Pol IV enzyme, it was expected that a lower accumulation of its transcripts would impair the accumulation of 24-nt siRNAs. We therefore generated libraries of small RNAs (electronic supplementary material, table S1, additional file 2) from leaves harvested at the same developmental stage on WT plantlets, the T0 and three T1 (T1-15, T1-17 and T1-23), sequenced them and compared the abundance of each size class between the libraries. Contrary to 24-nt siRNAs, the 21-nt classes were expected to be unimpacted in the RNAi lines. The siRNAs' abundances were thus normalized to those of 21-nt siRNAs in the WT library. As expected, we observed that the proportions of 24-nt siRNA abundances were lower in the T0 and all T1 libraries compared with the WT one (figure 2).

(d) The overall DNA methylation level is lowered in all three contexts, CG, CHG and CHH

As a consequence of impairing the accumulation of 24-nt small RNAs, an overall decrease in cytosine methylation was expected. To investigate this aspect, we profiled the whole genome DNA methylation of the T0 regenerant and two T1 individuals of its progeny (T1-15 and T1-23). We then examined the methylation differences between the RNAi lines and the WT on common sites that were available for all samples and found that the RNAi lines were globally hypomethylated in CHH context (figure 3), the hallmark of RdDM, but also in CG and CHG (electronic supplementary material, figure S3, additional file 1). Moreover, 10 subclasses of TEs were analysed across all samples and in all contexts and were found to be, on average, hypomethylated (figure 4).

(e) Some new insertions of known active TEs, but no generalized reactivation of transposition in *osnrpd1* RNAi lines

We initially hypothesized that *OsNRPD1* was a target of choice to broadly relax epigenetic control over TEs. We then try to systematically assess the transpositional activity in *osnrpd1* and compare it to WT plants. To identify and follow the inheritance of transposition events, we have generated, starting from the T1 plants described above, two more generations of single-seed descents. We thus obtained T2 and T3 generations from T1-15 and T1-23 (figure 5, top) and until T6 from T1-23. We thus resequenced the genomes of nine individuals, including the T0 as indicated in figure 5, using the Illumina-based paired-end technology. As a control, we resequenced the genome of the WT progenitor of the RNAi lines. All reads were mapped against the reference genome of *Oryza sativa* cv. Nipponbare.

We then used three different approaches, based on these alignments, to identify TEs' mobilization. They are briefly described here, and further details can be found in electronic supplementary material, additional file 6. We first used a candidate approach: *Tos17* and *Lullaby* are retrotransposons that have been previously shown to be mobilized both in *in vitro*-cultured cells and *in planta* in mutants impaired in methylation. Based on a simple visual analysis of the alignments in a genome browser (electronic supplementary material, figure S4, additional file 1), we identified 12 new insertions of *Tos17* and one new insertion of *Lullaby* in the T0 plant (figure 5). Some of them were still present in each of the three T1 plants (figure 5). All of them were confirmed by PCR (electronic supplementary material, figure S5, additional file 1) and sequencing. No new insertion was detected in the T1 and further generations except one insertion of *Tos17* (Tos17-13 in figure 5).

Secondly, these 14 insertions were used as a testing set to develop an algorithm to identify insertions of other elements. As depicted in electronic supplementary material, figure S6 (additional file 1), clipped and discordant alignments detected after short reads mapping against the reference genome were used to identify insertion sites and the TE at the origin of each insertion. The parameters of the programme were progressively fine-tuned until the whole set of *Tos17* and *Lullaby* insertions described above were identified and all false positives eliminated. In addition, many new insertions of a LINE element, *Karma*, were detected in one T1 and all other lines starting from the T2 and accumulating in the subsequent generations but not in the parental T0 plant (figure 5). No new insertion from any other TE was detected. Finally, we checked the uncovered neo-insertions by visual inspection of the alignments with a genome browser: we confirmed that all of them were present in the RNAi lines and that none of them were present in the WT progenitor of *osnrpd1*.

Finally, it is well known that short reads mapping is not adapted to the identification of insertions that occur in repetitive regions because this identification rests upon accurate alignments of reads at the insertion site, a prerequisite that is unreachable when the insertion occurs into repeats. To circumvent this problem, we tried to detect TEs that multiply in the genome without identifying their insertion site. We then developed another algorithm based on depth of coverage. Briefly, in a first step, we normalized the read coverage for each analysed genome by counting the number of reads aligned on a set of 59 unique genes (electronic supplementary material, table S2, additional file 4) and normalizing to the length of each gene (electronic supplementary material, table S3, additional file 4). In a second step, the reads aligned on each TE locus were counted and normalized to their length and to the number of reads corresponding to unique regions, giving an estimation of the copy number for each TE (electronic supplementary material, figure S7, additional file 1). This estimated copy number was obtained for the T0

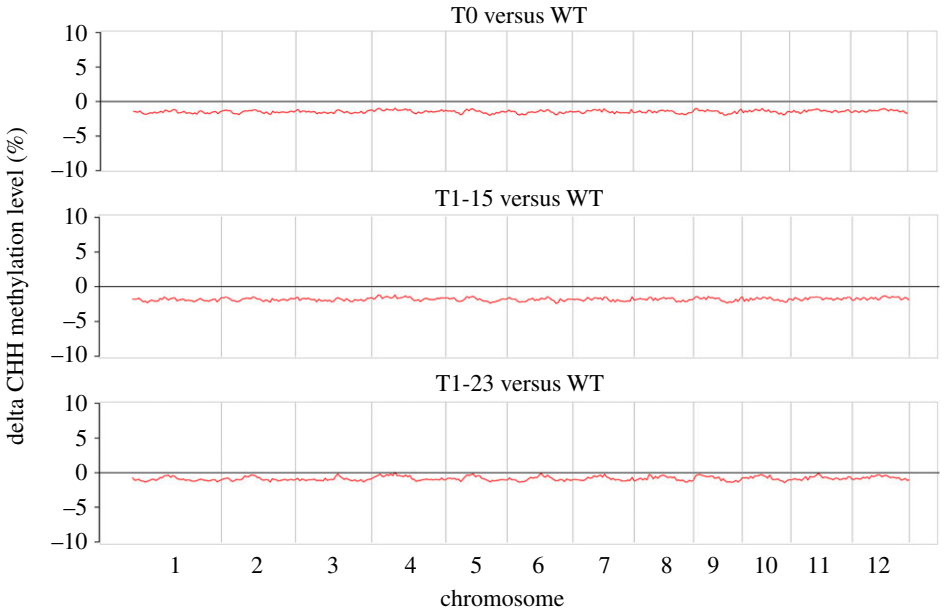

Figure 3. The whole genome level of CHH methylation is lower in the *osnrpd1* mutants. Genome-wide view of delta methylation in CHH context, showing that the T0 regenerant and both T1 progenies (T1-15 and T1-23) of the *osnrpd1* mutant have lower methylation than the wild-type (WT). Methylation in CHG and CG contexts is also affected as shown in electronic supplementary material, figure S3, additional file 1.

and the three T1 plants and compared to that of the WT. The method was first validated using the previously known copy number for *Tos17* and *Lullaby*. We then applied the strategy to the whole set of 295 LTR-RTs from our curated database. However, we could not detect a consistent increase in copy number for any of them (electronic supplementary material, table S4, additional file 4).

Therefore, we could not observe any *in planta* generalized reactivation of transposition in *osnrpd1*, except one *Tos17* insertion and the continuous retrotransposition, starting from the T2 generation, of the LINE-type TE called *Karma*. All other neo-insertions (i.e. detected in *osnrpd1* but not in the WT progenitor) were already present in the T0 regenerant from callus after transformation.

4. Discussion

In this paper, we have described the effects of a knock-down of the *OsNRPD1* gene in rice. The RNAi construct was effective because we could observe the targeting of the *OsNRPD1* gene with 21-nt siRNAs (electronic supplementary material, figure S2, additional file 1) and the reduction of the accumulation of *OsNRPD1* transcripts (figure 1). We then observed a reduction of the accumulation of 24-nt siRNAs (figure 2), an overall slight reduction of cytosine methylation in all contexts, CG, CHG and CHH (figures 3 and 4; electronic supplementary material, figure S3) and transposition of three retrotransposons, *Tos17*, *Lullaby* and *Karma*. However, the question arises whether we can attribute these effects to the knock-down of *OsNRPD1* because the construction of this RNAi line included an *in vitro* culture of cells that could explain at least part of them. It has indeed been shown that rice plants that were regenerated after prolonged tissue culture displayed both losses of methylation [38] and new insertions of *Tos17*, *Lullaby* and *Karma* [16–18]. Some observations may nevertheless indicate that the knock-down of *OsNRPD1* could enhance these effects.

First, we detected 12 new insertions of *Tos17* in the *osnrpd1* regenerant (T0 generation), when the average was 3.37 per line, and no more than 8, in a collection of 384 rice T-DNA mutants that had been obtained at the same facility, with the same protocol of transformation and callus culture [39]. In a WT background, where it was established that *Tos17* copy-number correlated with the duration of tissue culture, several months were necessary to reach such a level of transposition [16,40] when the transformation and regeneration process to obtain the *osnrpd1* regenerant only took seven weeks. A similar observation can be made for *Karma*: we have detected as many as five new insertions in a single T3 plant (T3-23 in figure 5) and 20 new others in three further generations (T6-23 in figure 5) when the original publication reported an average number of new insertions per plant of fewer than one [18]. It should be noted here that transposition events in the papers cited above were evaluated by hybridization after Southern blotting and not genome sequencing as reported here. However, we showed in a previous work that both methodologies identified the same number of *Tos17* insertions [41]. Therefore, this higher rate of transposition may be a sign of the effect of *OsNRPD1* knock-down.

Second, we detected a *Tos17* insertion in a T1 plant when it was absent from the analysed tissues (first leaves of a plantlet) of the parental T0 plant (Tos17-13 in figure 5 and electronic supplementary material, figure S5). To our knowledge, such an *in planta* transposition of *Tos17* has never previously been described in a WT background [16,40] but only in mutants impaired in methylation of DNA [23] or histones [21]. Similarly, this event may be interpreted as a transposition that occurred *in planta* in the T0 genome as a consequence of the *OsNRPD1* knock-down, at a late developmental stage, which have been transmitted to some individuals of the progeny.

If we assume that, based on these observations, part of the losses in methylation and transpositions events is the consequence of the knock-down of *OsNRPD1*, the effect of the latter is weak. An illustrative aspect is that we were not able to detect any other transposition events than those

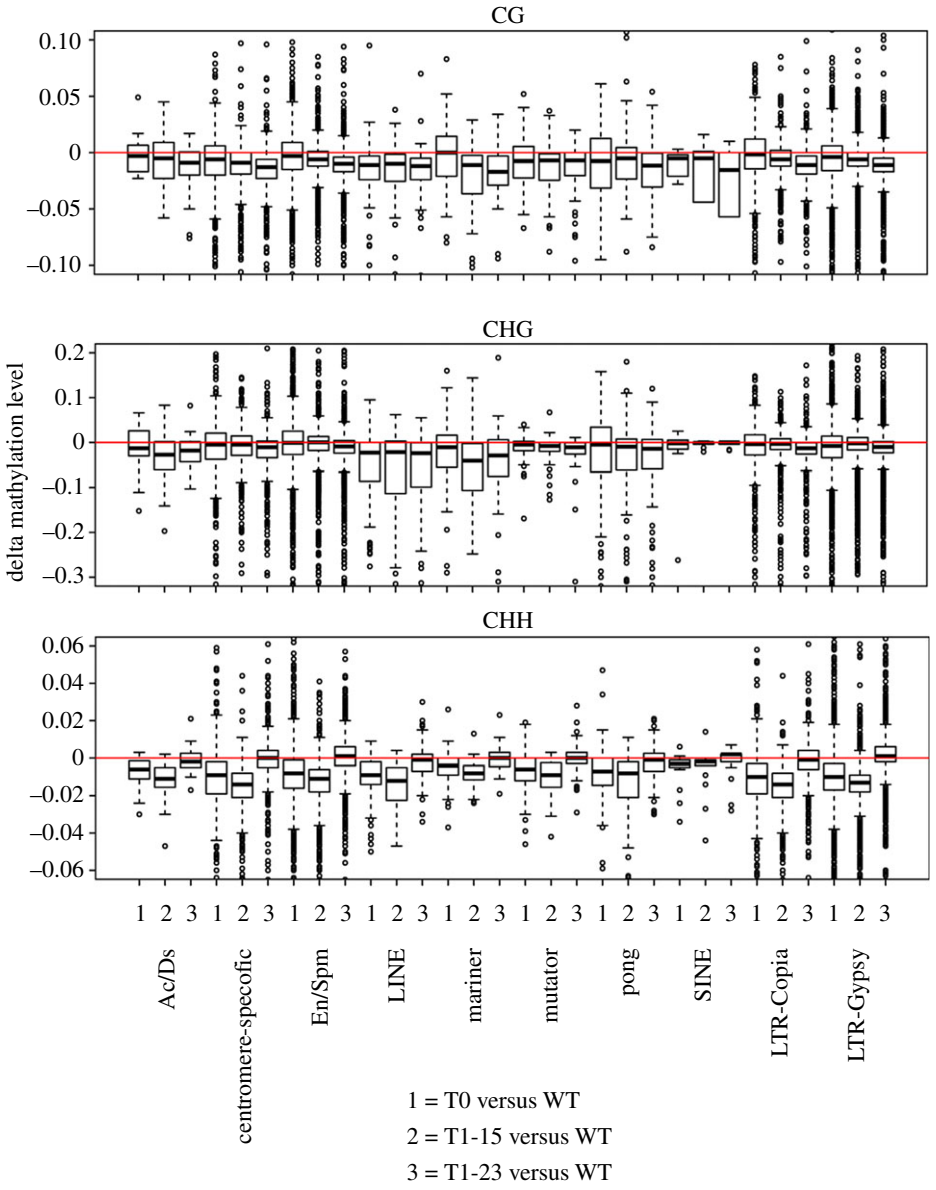

Figure 4. Methylation in 10 subclasses of transposons is lower in all contexts. To compare the methylation level distribution of differentially methylated transposable elements (DMTE) between each sample (T0, T1-15 and T1-23) and WT, we calculated the methylation differences of each DMTE between each sample and WT for 10 known classes of transposable elements and generated boxplots. The analysis has been done for cytosines in CG, CHG and CHH contexts, respectively, from top to bottom. For each class, the columns 1, 2 and 3 refer to the T0 versus WT comparison, the T1-15 versus WT comparison and the T1-23 versus WT comparison, respectively. The horizontal line indicates the level 0 of delta methylation (no change) all across each boxplot.

described above. This is in contrast to what has been reported for *oscmt3*, impaired in CHG methylation, where other TEs were found to be mobilized in addition to *Tos17* and *Lullaby* [23]. If we cannot rule out the possibility that transposition events have occurred that were not detected, it seems that *OsNRPD1* knock-down had a limited impact on transposition. This may be explained by a limited importance of *OsNRPD1* activity in that matter because this selective impact on transposition is reminiscent of what has been observed in *NRPD1* mutants of *A. thaliana* [37,42–44]. Similarly, the *osdcl3a* mutation, which reduced the expression of *OsDCL3* that encodes the rice DICER-LIKE 3 primarily responsible for 24-nt siRNA processing in canonical RdDM, reduced 24-nt siRNA predominantly from MITEs [26]. Although this study did not focus on transposition, this observation also underlined the selective release of the epigenetic control over TEs caused by the impairment of individual components of the RdDM machinery [45,46].

Alternatively, impairing canonical RdDM may not be sufficient to significantly affect methylation and trigger transposition. This would be explained by the existence in rice, as in *Arabidopsis*, of one or several non-canonical RdDM pathways [9,47] that could feed the canonical one downstream of Pol IV, or of parallel pathways independent of Pol IV. In *Arabidopsis*, it has indeed been shown that Pol II was involved in a silencing pathway, independent of Pol IV, that regulated DNA methylation at intergenic low-copy-number loci [48,49].

Finally and more probably, these limited effects are the result of the limited impact of the knock-down itself, raising the possibility, as discussed below, that a null mutant of *OsNRPD1* would be sterile. We indeed gathered several other indications that we only obtained weakly affected *osnrpd1* lines. The most obvious one is that we did not observe any clear developmental phenotype. Pol IV mutants in other species than *Arabidopsis*, whether mono- or dicotyledonous, display severe phenotypes. In maize, the *ZmRPD1* mutant

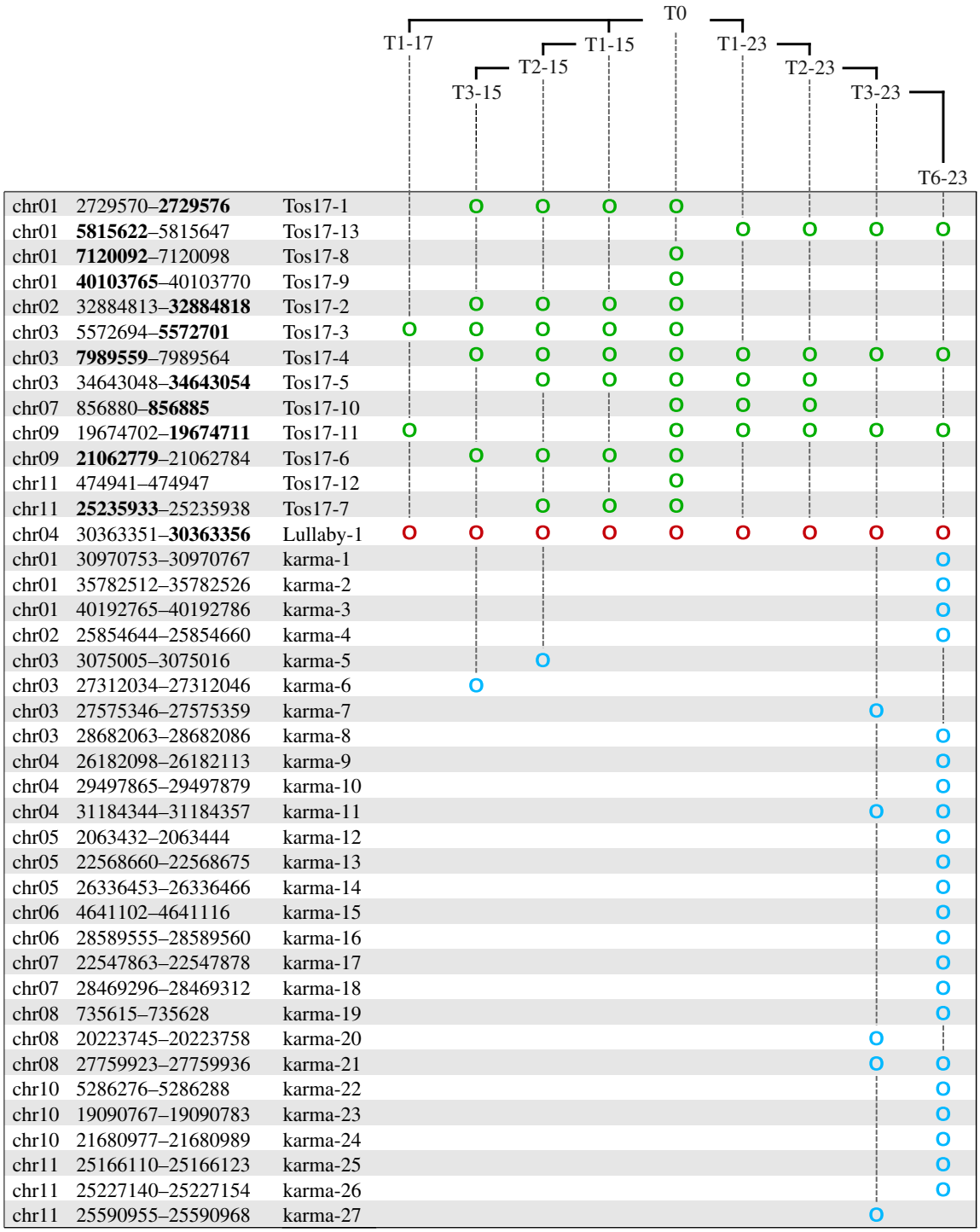

chr01	2729570–**2729576**	Tos17-1		o	o	o	o				
chr01	**5815622**–5815647	Tos17-13						o	o	o	o
chr01	**7120092**–7120098	Tos17-8					o				
chr01	**40103765**–40103770	Tos17-9					o				
chr02	32884813–**32884818**	Tos17-2		o	o	o	o				
chr03	5572694–**5572701**	Tos17-3	o	o	o	o	o				
chr03	**7989559**–7989564	Tos17-4		o	o	o	o	o	o	o	o
chr03	34643048–**34643054**	Tos17-5			o	o	o	o	o		
chr07	856880–**856885**	Tos17-10					o	o	o		
chr09	19674702–**19674711**	Tos17-11	o				o	o	o	o	o
chr09	**21062779**–21062784	Tos17-6		o	o	o	o				
chr11	474941–474947	Tos17-12					o				
chr11	**25235933**–25235938	Tos17-7			o	o	o				
chr04	30363351–**30363356**	Lullaby-1	o	o	o	o	o	o	o	o	o
chr01	30970753–30970767	karma-1									o
chr01	35782512–35782526	karma-2									o
chr01	40192765–40192786	karma-3									o
chr02	25854644–25854660	karma-4									o
chr03	3075005–3075016	karma-5			o						
chr03	27312034–27312046	karma-6		o							
chr03	27575346–27575359	karma-7								o	
chr03	28682063–28682086	karma-8									o
chr04	26182098–26182113	karma-9									o
chr04	29497865–29497879	karma-10									o
chr04	31184344–31184357	karma-11								o	o
chr05	2063432–2063444	karma-12									o
chr05	22568660–22568675	karma-13									o
chr05	26336453–26336466	karma-14									o
chr06	4641102–4641116	karma-15									o
chr06	28589555–28589560	karma-16									o
chr07	22547863–22547878	karma-17									o
chr07	28469296–28469312	karma-18									o
chr08	735615–735628	karma-19									o
chr08	20223745–20223758	karma-20								o	
chr08	27759923–27759936	karma-21								o	o
chr10	5286276–5286288	karma-22									o
chr10	19090767–19090783	karma-23									o
chr10	21680977–21680989	karma-24									o
chr11	25166110–25166123	karma-25									o
chr11	25227140–25227154	karma-26									o
chr11	25590955–25590968	karma-27								o	

Figure 5. List of all TEs insertions identified in *osnrpd1* mutants. The pedigree of all plants tested is indicated at the top. The three columns at the left of the table indicate the chromosome, the coordinates and the name of the new insertion. The coordinates are the start and end positions of the sequence that has been duplicated upon insertion as detected by our program. The true position of the insertion is one of them, depending of the orientation of the TE. For *Tos17* and *Lullaby* insertions, the positions highlighted in bold have been determined by sequencing. A circle (green for *Tos17*, red for *Lullaby*, blue for *Karma*) indicate the presence of the insertion in each plant.

called *rmr6* is pleiotropically affected in development [50,51]. Tilling mutants *braA.nrpd1* of *Brassica rapa* notably displayed asynchronous seed abortion [52]. Tomato *slnrpd1* null mutants have also been reported to be sterile [53]. Moreover, in contrast to *osnrpd1*, pleiotropic developmental abnormalities have been observed in mutants in other components of the RdDM pathway in rice, like *osdrm2* [24,27] and *osdcl3a* [26]. A strong *osnrpd1* mutant would, therefore, be expected to be affected the same way. In addition, an important reduction of genome-wide methylation was associated with those developmental defects. For instance, an 85% decrease in CHH methylation, 11% decrease in CG methylation and 20% decrease in CHG methylation were reported for *osdrm2* [27] when *osnrpd1* displayed less than 5% reduction in all contexts (figure 3 and electronic supplementary material, figure S3).

The fact that we likely obtained an RNAi line only slightly affected in *OsNRPD1* activity indicates, as previously suggested by others [30], that a null mutant would be sterile in rice. It is indeed surprising that a mutant of this central component of the RdDM machinery has never been described in such an important plant, as both a model species and a crop. Data are nevertheless available for other actors of

RdDM. The *osdrm2* null mutant, obtained by homologous recombination, is sterile [24]. The two described *osdcl3a* lines are knock-down RNAi lines, but they affect phenotypes with a severity correlated with the knock-down level of *OsDCL3a* [26], questioning the possibility of obtaining null mutants. Finally, we decided to target *OsNRPD1* by RNAi because we previously failed to find a viable insertional mutant in the available collections (EL, OP, 2014, unpublished data). We actually first focused on a T-DNA insertional mutation into the *OsNRDP1a* gene identified in the Oryza Tag Line library (http://oryzatagline.cirad.fr/, line AFVB01) based on the existence of a Flanking Sequence Tag (SAG8G10) corresponding to *OsNRPD1a*. However, we could not confirm the presence of any T-DNA at this position in the T2 plants that we could grow. Based on the recent demonstrations, as described above, that *NRPD1* null mutants in tomato and *Brassica* are sterile, it is therefore possible that this insertion gave rise to a sterile phenotype at the homozygous state in rice and that the seeds collected had segregated away this T-DNA. This hypothesis rests upon the speculation that *OsNRPD1b* could not complement the mutation. However, it would explain why no *nrdp1* knock-out mutant is available for rice, and that only weak mutants, like *osnrpd1* that we presented in this paper, may survive.

5. Conclusion

We have constructed a knock-down RNAi line of *OsNRPD1*, encoding the largest subunit of POLYMERASE IV, a central component of RdDM in rice. This line displayed reduced 24-nt siRNAs and DNA methylation compared to WT. We also detected new insertions of three retrotransposons. However, we could not clearly distinguish between the impact of *in vitro* culture and the knock-down of *OsNRPD1*, even if we have some indications of the effect of the latter. This may be explained by the fact that we only obtained a weakly affected line. We propose reasons that support the hypothesis of the sterility of a null mutant of *OsNRPD1*.

Data accessibility. Seeds of *osnrpd1* lines are available from the corresponding author on reasonable request. Scripts to identify TEs insertions are available at github (https://github.com/EricUPVD/sam2ins) under the Unlicence, a license with no conditions. Sequences have been deposited at NCBI under the SRA bioproject accession PRJNA535389. All other relevant data have been provided within the main text, figures and additional files.

Authors' contributions. E.D. generated the plant material and conducted all experiments and bioinformatics analysis related to OsNRDP1 expression and TEs mobilization under the supervision of O.P. and E.L. T.-F.L., Y.-J.H. and J.-H.L. did the BS-Seq and methylome analysis under the supervision of P.-Y.C. S.M.M. did the sRNA-seq analysis under the supervision of B.C.M. C.L. and D.P. did the PCR validations of TEs insertions under the supervision of E.D. M.-C.C and C.L. performed the RNA-seq analysis. D.M. and E.G. constructed the initial *osnrpd1* RNAi line. E.L. supervised the work, wrote the scripts to identify TEs insertions and wrote the manuscript. All authors read and approved the final manuscript.

Competing interests. We declare we have no competing interests.

Funding. Emilie Debladis was supported by a grant from the French Ministry of Education. The funding body had no role in the design of the study, analysis and interpretation of data nor in writing the manuscript.

Acknowledgements. We thank Moloya Gohain and Pearl chang for the preliminary analysis of rice methylome, Edouard Jobet for the RT-qPCR analysis, Mayumi Nakano for assistance with data handling and Moaine Elbaidouri for critical reading of the manuscript.

References

1. Feschotte C, Pritham EJ. 2007 DNA transposons and the evolution of eukaryotic genomes. *Annu. Rev. Genet.* **41**, 331–368. (doi:10.1146/annurev.genet.40.110405.090448)
2. Wicker T *et al.* 2007 A unified classification system for eukaryotic transposable elements. *Nat. Rev. Genet.* **8**, 973. (doi:10.1038/nrg2165)
3. Schulman AH. 2013 Retrotransposon replication in plants. *Curr. Opin. Virol.* **3**, 604–614. (doi:10.1016/j.coviro.2013.08.009)
4. Lisch D. 2013 How important are transposons for plant evolution? *Nat. Rev. Genet.* **14**, 49–61. (doi:10.1038/nrg3374)
5. Bennetzen JL, Wang H. 2014 The contributions of transposable elements to the structure, function, and evolution of plant genomes. *Annu. Rev. Plant Biol.* **65**, 505–530. (doi:10.1146/annurev-arplant-050213-035811)
6. Mita P, Boeke JD. 2016 How retrotransposons shape genome regulation. *Curr. Opin. Genet. Dev.* **37**, 90–100. (doi:10.1016/j.gde.2016.01.001)
7. Deng X, Song X, Wei L, Liu C, Cao X. 2016 Epigenetic regulation and epigenomic landscape in rice. *Natl Sci. Rev.* **3**, 309–327. (doi:10.1093/nsr/nww042)
8. Matzke MA, Mosher RA. 2014 RNA-directed DNA methylation: an epigenetic pathway of increasing complexity. *Nat. Rev. Genet.* **15**, 394–408. (doi:10.1038/nrg3683)
9. Cuerda-Gil D, Slotkin RK. 2016 Non-canonical RNA-directed DNA methylation. *Nat. Plants* **2**, 16163. (doi:10.1038/nplants.2016.163)
10. Cao X, Aufsatz W, Zilberman D, Mette MF, Huang MS, Matzke M, Jacobsen SE. 2003 Role of the DRM and CMT3 methyltransferases in RNA-directed DNA methylation. *Curr. Biol.* **13**, 2212–2217. (doi:10.1016/j.cub.2003.11.052)
11. Law JA, Jacobsen SE. 2010 Establishing, maintaining and modifying DNA methylation patterns in plants and animals. *Nat. Rev. Genet.* **11**, 204. (doi:10.1038/nrg2719)
12. Fultz D, Choudury SG, Slotkin RK. 2015 Silencing of active transposable elements in plants. *Curr. Opin. Plant Biol.* **27**(Suppl. C), 67–76. (doi:10.1016/j.pbi.2015.05.027)
13. International Rice Genome Sequencing Project. 2005 The map-based sequence of the rice genome. *Nature* **436**, 793. (doi:10.1038/nature03895)
14. Naito K, Cho E, Yang G, Campbell MA, Yano K, Okumoto Y, Tanisaka T, Wessler SR. 2006 Dramatic amplification of a rice transposable element during recent domestication. *Proc. Natl Acad. Sci. USA* **103**, 17 620–17 625. (doi:10.1073/pnas.0605421103)
15. Petit J *et al.* 2009 Diversity of the Ty-1 copia retrotransposon *Tos17* in rice (*Oryza sativa* L.) and the AA genome of the *Oryza* genus. *Mol. Genet. Genom.* **282**, 633–652. (doi:10.1007/s00438-009-0493-z)
16. Hirochika H, Sugimoto K, Otsuki Y, Tsugawa H, Kanda M. 1996 Retrotransposons of rice involved in mutations induced by tissue culture. *Proc. Natl Acad. Sci. USA* **93**, 7783–7788. (doi:10.1073/pnas.93.15.7783)
17. Picault N *et al.* 2009 Identification of an active LTR retrotransposon in rice. *Plant J.* **58**, 754–765. (doi:10.1111/j.1365-313X.2009.03813.x)
18. Komatsu M, Shimamoto K, Kyozuka J. 2003 Two-step regulation and continuous retrotransposition of the rice LINE-type retrotransposon *Karma*. *Plant Cell* **15**, 1934–1944. (doi:10.1105/tpc.011809)
19. Jiang N, Bao Z, Zhang X, Hirochika H, Eddy SR, McCouch SR, Wessler SR. 2003 An active DNA transposon family in rice. *Nature* **421**, 163. (doi:10.1038/nature01214)
20. Kikuchi K, Terauchi K, Wada M, Hirano H-Y. 2003 The plant MITE *mPing* is mobilized in anther culture. *Nature* **421**, 167. (doi:10.1038/nature01218)
21. Ding Y *et al.* 2007 SDG714, a histone H3K9 methyltransferase, is involved in *Tos17* DNA

methylation and transposition in rice. *Plant Cell* **19**, 9–22. (doi:10.1105/tpc.106.048124)

22. La H *et al.* 2011 A 5-methylcytosine DNA glycosylase/lyase demethylates the retrotransposon *Tos17* and promotes its transposition in rice. *Proc. Natl Acad. Sci. USA* **108**, 15 498–15 503. (doi:10.1073/pnas.1112704108)
23. Cheng C, Tarutani Y, Miyao A, Ito T, Yamazaki M, Sakai H, Fukai E, Hirochika H. 2015 Loss of function mutations in the rice chromomethylase OsCMT3a cause a burst of transposition. *Plant J.* **83**, 1069–1081. (doi:10.1111/tpj.12952)
24. Moritoh S, Eun C-H, Ono A, Asao H, Okano Y, Yamaguchi K, Shimatani Z, Koizumi A, Terada R. 2012 Targeted disruption of an orthologue of *DOMAINS REARRANGED METHYLASE 2*, *OsDRM2*, impairs the growth of rice plants by abnormal DNA methylation. *Plant J.* **71**, 85–98. (doi:10.1111/j.1365-313X.2012.04974.x)
25. Hu L *et al.* 2014 Mutation of a major CG methylase in rice causes genome-wide hypomethylation, dysregulated genome expression, and seedling lethality. *Proc. Natl Acad. Sci. USA* **111**, 10 642–10 647. (doi:10.1073/pnas.1410761111)
26. Wei L *et al.* 2014 Dicer-like 3 produces transposable element-associated 24-nt siRNAs that control agricultural traits in rice. *Proc. Natl Acad. Sci. USA* **111**, 3877–3882. (doi:10.1073/pnas.1318131111)
27. Tan F, Zhou C, Zhou Q, Zhou S, Yang W, Zhao Y, Li G, Zhou D-X. 2016 Analysis of chromatin regulators reveals specific features of rice DNA methylation pathways. *Plant Physiol.* **171**, 2041–2054. (doi:10.1104/pp.16.00393)
28. Zhou M, Law JA. 2015 RNA Pol IV and V in gene silencing: rebel polymerases evolving away from Pol II's rules. *Curr. Opin. Plant Biol.* **27**, 154–164. (doi:10.1016/j.pbi.2015.07.005)
29. Huang Y *et al.* 2015 Ancient origin and recent innovations of RNA polymerase IV and V. *Mol. Biol. Evol.* **32**, 1788–1799. (doi:10.1093/molbev/msv060)
30. Arikit S, Zhai J, Meyers BC. 2013 Biogenesis and function of rice small RNAs from non-coding RNA precursors. *Curr. Opin. Plant Biol.* **16**, 170–179. (doi:10.1016/j.pbi.2013.01.006)
31. Sallaud C *et al.* 2003 Highly efficient production and characterization of T-DNA plants for rice (*Oryza sativa* L.) functional genomics. *Theor. Appl. Genet.* **106**, 1396–1408. (doi:10.1007/s00122-002-1184-x)
32. Debladis E, Llauro C, Carpentier M-C, Mirouze M, Panaud O. 2017 Detection of active transposable elements in *Arabidopsis thaliana* using Oxford Nanopore Sequencing technology. *BMC Genom.* **18**, 537. (doi:10.1186/s12864-017-3753-z)
33. Langmead B, Salzberg SL. 2012 Fast gapped-read alignment with Bowtie 2. *Nat. Methods* **9**, 357–359. (doi:10.1038/nmeth.1923)
34. Li H *et al*. 2009 The Sequence Alignment/Map format and SAMtools. *Bioinformatics* **25**, 2078–2079. (doi:10.1093/bioinformatics/btp352)
35. Urich MA, Nery JR, Lister R, Schmitz RJ, Ecker JR. 2015 MethylC-seq library preparation for base-resolution whole-genome bisulfite sequencing. *Nat. Protoc.* **10**, 475–483. (doi:10.1038/nprot.2014.114)
36. Guo W, Fiziev P, Yan W, Cokus S, Sun X, Zhang MQ, Chen P-Y, Pellegrini M. 2013 BS-Seeker2: a versatile aligning pipeline for bisulfite sequencing data. *BMC Genom.* **14**, 774. (doi:10.1186/1471-2164-14-774)
37. Pontier D *et al.* 2005 Reinforcement of silencing at transposons and highly repeated sequences requires the concerted action of two distinct RNA polymerases IV in *Arabidopsis*. *Genes Dev.* **19**, 2030–2040. (doi:10.1101/gad.348405)
38. Stroud H, Ding B, Simon SA, Feng S, Bellizzi M, Pellegrini M, Wang G-L, Meyers BC, Jacobsen SE. 2013 Plants regenerated from tissue culture contain stable epigenome changes in rice. *Elife* **2**, e00354. (doi:10.7554/eLife.00354)
39. Piffanelli P *et al.* 2007 Large-scale characterization of Tos17 insertion sites in a rice T-DNA mutant library. *Plant Mol. Biol.* **65**, 587–601. (doi:10.1007/s11103-007-9222-3)
40. Hirochika H. 2001 Contribution of the *Tos17* retrotransposon to rice functional genomics. *Curr. Opin. Plant Biol.* **4**, 118–122. (doi:10.1016/S1369-5266(00)00146-1)
41. Sabot F *et al.* 2011 Transpositional landscape of the rice genome revealed by paired-end mapping of high-throughput re-sequencing data. *Plant J.* **66**, 241–246. (doi:10.1111/j.1365-313X.2011.04492.x)
42. Onodera Y, Haag JR, Ream T, Nunes PC, Pontes O, Pikaard CS. 2005 Plant Nuclear RNA polymerase IV mediates siRNA and DNA methylation-dependent heterochromatin formation. *Cell* **120**, 613–622. (doi:10.1016/j.cell.2005.02.007)
43. Kanno T, Huettel B, Mette MF, Aufsatz W, Jaligot E, Daxinger L, Kreil DP, Matzke M, Matzke AJM. 2005 Atypical RNA polymerase subunits required for RNA-directed DNA methylation. *Nat. Genet.* **37**, 761. (doi:10.1038/ng1580)
44. Herr AJ, Jensen MB, Dalmay T, Baulcombe DC. 2005 RNA polymerase IV directs silencing of endogenous DNA. *Science* **308**, 118–120. (doi:10.1126/science.1106910)
45. Lippman Z, May B, Yordan C, Singer T, Martienssen R. 2003 Distinct mechanisms determine transposon inheritance and methylation via small interfering RNA and histone modification. *PLoS Biol.* **1**, e67. (doi:10.1371/journal.pbio.0000067)
46. Rigal M, Mathieu O. 2011 A 'mille-feuille' of silencing: epigenetic control of transposable elements. *Biochim. Biophys. Acta* **1809**, 452–458. (doi:10.1016/j.bbagrm.2011.04.001)
47. Matzke MA, Kanno T, Matzke AJM. 2015 RNA-directed DNA methylation: the evolution of a complex epigenetic pathway in flowering plants. *Annu. Rev. Plant Biol.* **66**, 243–267. (doi:10.1146/annurev-arplant-043014-114633)
48. Stroud H, Greenberg MVC, Feng S, Bernatavichute YV, Jacobsen SE. 2013 Comprehensive analysis of silencing mutants reveals complex regulation of the *Arabidopsis* methylome. *Cell* **152**, 352–364. (doi:10.1016/j.cell.2012.10.054)
49. Zheng B, Wang Z, Li S, Yu B, Liu J-Y, Chen X. 2009 Intergenic transcription by RNA Polymerase II coordinates Pol IV and Pol V in siRNA-directed transcriptional gene silencing in *Arabidopsis*. *Genes Dev.* **23**, 2850–2860. (doi:10.1101/gad.1868009)
50. Erhard KF, Stonaker JL, Parkinson SE, Lim JP, Hale CJ, Hollick JB. 2009 RNA polymerase IV functions in paramutation in *Zea mays*. *Science* **323**, 1201–1205. (doi:10.1126/science.1164508)
51. Parkinson SE, Gross SM, Hollick JB. 2007 Maize sex determination and abaxial leaf fates are canalized by a factor that maintains repressed epigenetic states. *Dev. Biol.* **308**, 462–473. (doi:10.1016/j.ydbio.2007.06.004)
52. Grover JW, Kendall T, Baten A, Burgess D, Freeling M, King GJ, Mosher RA. 2018 Maternal components of RNA-directed DNA methylation are required for seed development in *Brassica rapa*. *Plant J.* **94**, 575–582. (doi:10.1111/tpj.13910)
53. Gouil Q, Baulcombe DC. 2016 DNA methylation signatures of the plant chromomethyltransferases. *PLoS Genet.* **12**, e1006526. (doi:10.1371/journal.pgen.1006526)